On the inadequacy of Stern-Volmer and FRET in describing quenching in binary donor-acceptor solutions ⊘

Special Collection: 40 Years of Colloidal Nanocrystals in JCP

Xuanheng Tan (); Justin R. Caram (



J. Chem. Phys. 158, 204705 (2023) https://doi.org/10.1063/5.0148170





CrossMark

AIP Publishing







On the inadequacy of Stern-Volmer and FRET in describing quenching in binary donor-acceptor solutions

Cite as: J. Chem. Phys. 158, 204705 (2023); doi: 10.1063/5.0148170 Submitted: 28 February 2023 • Accepted: 8 May 2023 • Published Online: 23 May 2023







Xuanheng Tan D and Justin R. Caram Do



AFFILIATIONS

Department of Chemistry and Biochemistry, University of California, Los Angeles, 607 Charles E. Young Drive, Los Angeles, California 90095-1569, USA

Note: This paper is part of the JCP Special Topic on 40 Years of Colloidal Nanocrystals in JCP.

^{a)}Author to whom correspondence should be addressed: jcaram@chem.ucla.edu

ABSTRACT

Quantitative fluorescence quenching is a common analytical approach to studying the mechanism of chemical reactions. The Stern-Volmer (S-V) equation is the most common expression used to analyze the quenching behavior and can be used to extract kinetics in complex environments. However, the approximations underlying the S-V equation are incompatible with Förster Resonance Energy Transfer (FRET) acting as the primary quenching mechanism. The nonlinear distance dependence of FRET leads to significant departures from "standard" S-V quenching curves, both by modulating the interaction range of donor species and by increasing the effect of component diffusion. We demonstrate this inadequacy by probing the fluorescence quenching of long-lifetime lead sulfide quantum dots mixed with plasmonic covellite copper sulfide nanodisks (NDs), which serve as perfect fluorescent quenchers. By applying kinetic Monte Carlo methods, which consider particle distributions and diffusion, we are able to quantitatively reproduce experimental data, which show significant quenching at very small concentrations of NDs. The distribution of interparticle distances and diffusion are concluded to play important roles in fluorescence quenching, particularly in the shortwave infrared, where photoluminescent lifetimes are often long relative to diffusion time scales.

Published under an exclusive license by AIP Publishing. https://doi.org/10.1063/5.0148170

I. INTRODUCTION

Proposed in 1919 by Otto Stern and Max Volmer, the Stern-Volmer model quantitatively described the decrease in the fluorescence intensity of emitters in the presence of quenchers, molecules that are capable of bringing the excited emitters back to ground states. The linear relationship shown in a Stern-Volmer (S-V) plot between quenching ratio and quencher concentrations is often attributed to the collisions between emitters and quenchers. For this reason, the Stern-Volmer model is usually referred to as collisional quenching and is associated with measuring rate constants. Deviation from the linear Stern-Volmer law usually implies some factors other than collisional quenching, including attraction between particles, pre-formation of complexes, or incomplete quenching.

While collisional quenching is treated in the Stern-Volmer formalism, Förster resonance energy transfer (FRET) is another process that can deplete the excited state of a donor molecule. In

FRET, dipole-dipole interactions result in energy migration from the donor to the acceptor, provided that the emission of the donor overlaps with the absorption of the acceptor. FRET rates depend in a known non-linear fashion on the distance between the donor and acceptor and, thus, can be inverted to experimentally determine the intramolecular distance (or distribution of distances) between each species. In a single molecule context, FRET is a powerful tool to deduce structural changes in polymers induced by folding or selfassembly, among many other applications. 7-11 In ensemble contexts, Inokuti and Hirayama gave a generalized treatment of fluorescence quenching in crystals by comparing summed rates of energy transfer from donors to acceptors and decay rates of excited donors.¹² This treatment is useful for excitonic crystals but has clear limitations in mixtures where the distribution is more complex and changing over

Surprisingly, despite considerable examples of fluorescent quenching due to FRET, there exists no analytical expression that predicts quenching rate as a function of donor and acceptor

concentration and FRET overlap in dilute mixtures of noninteracting particles. By simple inspection, while the collisional S-V rate of quenching depends linearly on the concentration of the quencher, in FRET, the rate also depends on the interparticle distance ($\sim r^{-6}$). Given that the interparticle distance is approximately given by $r \sim n^{-1/3}$, where *n* is the number density, one might expect that the quenching rate will vary with n^2 or quadratically with number density. Such a mechanism may lead to significant quenching of photoluminescence in the case of small impurities or could be used as a method to probe analyte concentration in a biochemical assay, but only if the proper form is used. It is worth noting, however, that there is no analytic expression of the distinct interparticle distance distribution for even hard-sphere binary mixtures, complicating the development of a single equation that takes in concentration, transition dipole, and lifetime and predicts quenching efficiency. 13-17

In this work, we study the energy transfer between short-wavelength infrared (SWIR) emitters and plasmonic nanoparticles. We synthesized lead sulfide (PbS) quantum dots (QDs) and plasmonic covellite copper sulfide (CuS) nanodisks (NDs) before mixing them in a colloidal solution. These form an ideal FRET pair for exploring the effects of diffusion and energy transfer in dilute solutions, as the CuS nanodisks have a complete overlap with the emission spectrum of the PbS but do not interfere (shadow) our PbS absorption spectra. The relatively long lifetime of PbS also allows us to explore the role of diffusion in energy quenching. Given that many SWIR emitters have long lifetimes (e.g., quantum dots and lanthanide nanoparticles), the role of diffusion is highly pertinent to the dynamics of quenching in this spectral window.

Our experiments revealed a high degree of quenching at very low concentrations of CuS NDs, accompanied by a non-linear dependence between the quenching ratio and concentrations of plasmonic CuS NDs, which cannot be explained by the conventional Stern–Volmer modeling. We simulate several potential explanations to describe these results, exploring the role of interparticle distance distribution, nonlinear FRET rates, and diffusion, and reach quantitative agreement with experiments using kinetic Monte Carlo (kMC) simulations that account for all effects. We conclude by discussing how Stern–Volmer descriptions of quenching are highly inadequate in describing FRET pairs in systems with large FRET radii and/or long lifetimes and concomitant large diffusion lengths.

II. RESULTS AND DISCUSSIONS

We synthesized PbS QDs and CuS NDs as the model emitters and quenchers through traditional colloidal methods (see the supplementary material for details). The absorption spectroscopy of CuS NDs shows a plasmonic peak in the SWIR region [Fig. 1(a)] consistent with prior reports. ^{18,19} For PbS QDs, the PL spectroscopy of PbS QDs shows a close resonance of the emission peak with the plasmonic absorption peak of CuS NDs [Fig. 1(a)]. The morphology of the as-synthesized nanocrystals is confirmed by TEM images, where spherical PbS QDs and hexagonal CuS NDs are clearly identified [Fig. 1(b)]. PbS QDs are measured to have an average radius of 3.6 nm, and CuS NDs are measured to have an average diagonal length of 19 nm and an average thickness of 5.0 nm (see the supplementary material, Figs. S1 and S2). The absorption trace of

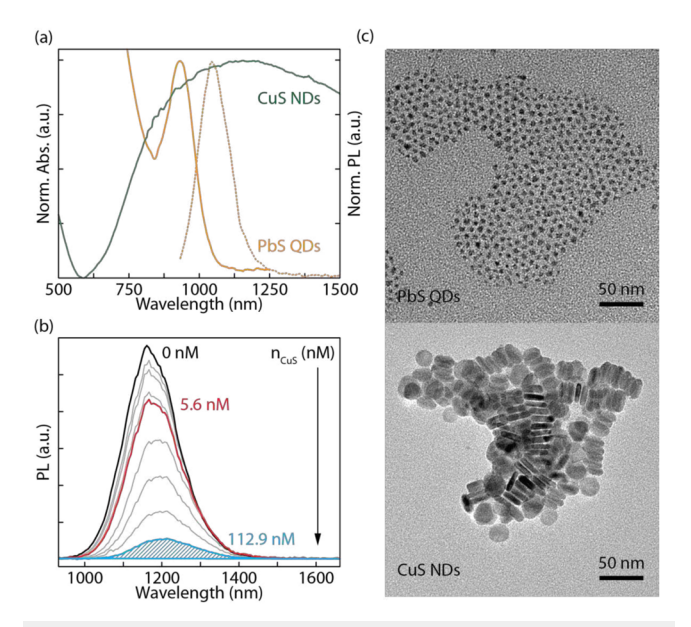


FIG. 1. a) Normalized absorbance (solid lines) and PL (dashed line) spectra of the synthesized PbS QDs (orange) and CuS NDs (green). (b) TEM images of the synthesized PbS QDs (top) and CuS NDs (bottom). (c) PL traces of PbS QDs in one group of titration experiments with CuS NDs. The shaded area under the curve of a PL trace is considered as PL intensity and used to determine quenching ratios.

CuS NDs and the PL trace of PbS QDs are used to calculate the spectral overlap, which is required to calculate the FRET radius. From TEM images, size parameters of PbS QDs and CuS NDs are measured and used to calculate the diffusion coefficients of nanocrystals using the Stokes–Einstein equation. The concentrations of PbS QDs are determined using the sizing curve and extinction coefficients reported by Moreels *et al.*, and the concentrations of CuS NDs are estimated from a synthetic procedure and the corresponding extinction coefficient is extracted using the Beer–Lambert law. These parameters are then used for all modeling and simulations (Table I). The TEM of the mixture confirmed no interaction between PbS and CuS samples (see the supplementary material, Fig. S3).

To study the fluorescence quenching of emissive nanocrystals by using plasmonic nanocrystals in the SWIR region, a series of titration experiments of PbS QDs with CuS NDs were performed (see the supplementary material for details). The steady-state PL spectroscopy clearly shows a continuous decrease in fluorescence intensities of PbS QDs upon serial addition of CuS NDs [see Fig. 1(c) for one example trace]. Note that due to the relatively high absorptivity of CuS NDs, the secondary inner filter effect introduced by the absorption of CuS NDs was accounted for and the corrected PL intensities were used to calculate the quenching ratio (see the supplementary material for details). Another direct evidence of the quenching is demonstrated by time-resolved PL measurements, where an obvious decrease in the donor lifetimes is observed (see the supplementary material, Tables S1 and S2).

The results of fluorescence quenching in titration experiments show consistent patterns across the range of emitter concentrations tested [Fig. 2(a)]. We first observe that changing quencher

TABLE I. Parameters used in modeling and simulations.

Nanocrystals	Size ^a (nm)	Concentration ^b (µM)	Diffusion coefficient (nm ² ⋅ns ⁻¹)	Total decay rate (ns ⁻¹)	FRET radius (nm)
PbS QDs	3.6 ± 0.7	$33.7 \pm 3.1^{\circ}$	0.22 ± 0.04	0.000 45 ^d	
CuS NDs	5.0 ± 1.2 19.0 ± 9.0	0.36 ^e	$0.048 \pm 0.005^{\mathrm{f}}$		17.40 ± 0.20

^aMeasured from statistics of TEM images (see the supplementary material, Figs. S1 and S2). For PbS QDs, the diameter is reported; For CuS NDs, the thickness (top row) and diagonal length (bottom row) are reported.

^fCalculated using the corrected hydrodynamic radius due to non-spherical shape.²

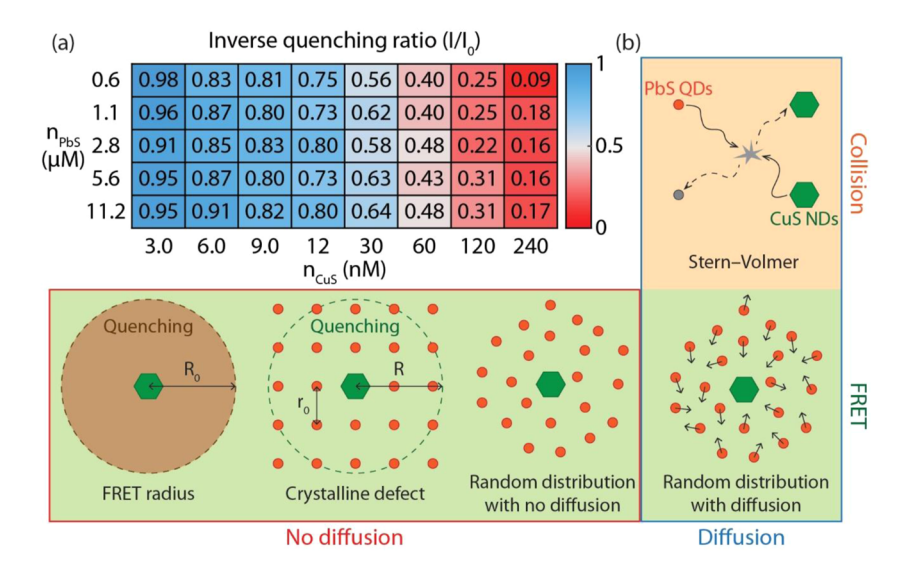


FIG. 2. (a) A heatmap of inverse quenching ratios for all conditions of titration experiments (see also Fig. S7). The inverse quenching ratios have been corrected for the inner filter effect. (b) A diagram of explored models in modeling and simulations. The models can be categorized into quenching by FRET (green background) and collisional quenching (orange background) based on the mechanism of energy transfer responsible for quenching, or into models considering diffusion (blue frame) and without considering diffusion (orange frame). The PL of excited PbS QDs (orange circles) are quenched by plasmonic CuS NDs (green hexagons), resulting in de-excited PbS QDs (gray circles)

concentration has the largest effect, consistent with it being the limiting quenching "reagent." Second, all the quencher concentrations experimented in the titrations were on a nanomolar scale, which is significantly low given such a high degree of quenching (up to 91% extinction) compared to other reported emitter–quencher pairs, including pairs of nanoparticles, pairs of fluorescent proteins, pairs of dye molecules, pairs of amino acids, dye molecule–DNA pairs, and quantum dot–fluorescent protein pairs, which typically only display quenching at micromolar concentrations. ^{24–29} Second, besides the high quenching efficiency at low quencher concentrations, a non-linear relationship between quenching ratios and quencher concentrations is also observed. These patterns suggest that additional complexity is not accounted for in S–V quenching for the PbS QDs–CuS NDs pair in the SWIR region.

A. Comparison to analytical and simulated quenching behavior

To explain the quenching patterns observed in experiments, we explored several models and compared them to our experimental results [Fig. 2(b)]. They are enumerated and described in Sec. II A.

1. Collisional quenching (Stern-Volmer)

In the Stern–Volmer model, the cause of fluorescence quenching is attributed to collisions between emitters and quenchers. As a result, the relationship between the quenching ratio and the number density of quenchers (n_{CuS}) is given by

$$\frac{I_0}{I} = 1 + \frac{k_q}{k_0} n_{CuS},\tag{1}$$

where k_q is the quenching rate and k_0 is the total decay rate of emitters without quenchers. Under this quenching scheme, a linear dependence is typically observed when k_q remains constant, which is indicative of a diffusion-limited collisional reaction between emitters and quenchers. The maximum possible quenching rate k_q is given by the maximum collision rate for diffusing particles,

$$k_q = 4\pi DR_C, (2)$$

where D is the sum of the diffusion coefficients of the emitter and quencher and R_C is the sum of the contact radius of the emitter and quencher (for PbS QDs: radius; for CuS NDs: $^{1}/_{2}$ of thickness), representing spontaneous reaction upon any collision. 30

^bFor stock solutions

^cCalculated using the size-independent absorption coefficient.²²

^dMeasured in time-resolved PL spectroscopy (see the supplementary material, Fig. S8).

^eEstimated from the synthetic procedure of CuS NDs (see the supplementary material for details).

2. Quenching by FRET

Fluorescence quenching is fundamentally an energy transfer process between a donor and an acceptor. If the quenching process is FRET mediated, it is based on dipole–dipole interactions in each species. The FRET rate depends non-linearly on the distance between emitters and quenchers (r),

$$k_{FRET} = k_0 \left(\frac{R_0}{r}\right)^6,\tag{3}$$

where R_0 is defined as the Förster distance. We will consider several ways that FRET can be introduced into a Stern–Volmer style equation.

a. FRET radius as effective quenching volume. The FRET radius R_0 is calculated by the following equation:

$$R_0^6 = 8.785 \times 10^{-5} \frac{\kappa^2 \phi_D J}{n^4},\tag{4}$$

where κ^2 is the dipole orientation factor, ϕ_D is the quantum yield of emitters, and n is the refractive index of solvent. The spectral overlap J is defined as

$$J = \frac{\int F_D(\lambda)\varepsilon_A(\lambda)\lambda^4 d\lambda}{\int F_D(\lambda)d\lambda},\tag{5}$$

where $F_D(\lambda)$ is the emission spectrum of emitters and $\varepsilon_A(\lambda)$ is the molar extinction coefficient of quenchers. 20 R_0 clearly depends only on the spectral properties of the emitter and quencher, requiring no knowledge of the concentrations. For large molecules, such as polymers or proteins, intramolecular interchromophore distance (r) can be determined by measuring the FRET efficiency (E_{FRET}) through spectroscopy.

$$E_{FRET} = \frac{I}{I_0} = \frac{k_0}{k_0 + k_{FRET}} = \frac{1}{1 + \left(\frac{R_0}{a}\right)^6},$$
 (6)

where a 50% of FRET efficiency is achieved at an emitter-quencher distance equal to the FRET radius. We apply this idea of associating fluorescence quenching with only the FRET radius to the mixture of PbS QDs and CuS NDs. Assuming that the fluorescence of half of the emitters within the range of the FRET radius is completely quenched, the quenching ratio would be given by a pseudo-Stern-Volmer relation,

$$\frac{I_0}{I} = 1 + \frac{n_{PbS} \cdot \frac{1}{2} \cdot \frac{4\pi R_0^3}{3} \cdot n_{CuS}V}{n_{PbS}V} = 1 + \frac{2\pi R_0^3}{3}n_{CuS}.$$
 (7)

This is the equivalent of creating a quenched volume.

b. Crystalline defect. One of the fundamental reasons that FRET efficiency measurements can be used to determine the interchromophore distance is that the variance of this intramolecular distance in the ensemble is relatively small. ^{31,32} For a mixture where emitters and quenchers are two different species in solution, the distance distribution is much larger and cannot be neglected. ^{16,33,34} To account for this, we add a layer of complexity on top of the "FRET

radius only" calculation by introducing a crystalline distribution of interparticle distances, where CuS NDs are considered to be evenly distributed in a lattice of PbS QDs, and every PbS QDs are allowed to transferring energies only to the nearest CuS NDs. The quenching ratio is then calculated by comparing the total FRET rate and the total decay rate in the ensemble,

$$\frac{I_0}{I} = 1 + \frac{\int_{r_0}^R k_0 \left(\frac{R_0}{r}\right)^6 \cdot 4\pi r^2 n_{PbS} dr}{k_0 \frac{4\pi R^3}{3} n_{PbS}},$$
 (8)

where the total FRET rate is calculated by integrating rates over all possible interparticle distances. The limits of the distance are determined given the number densities of PbS QDs and CuS NDs,

$$\frac{1}{n_{PbS}} = r_0^3; \quad \frac{1}{n_{CuS}} = \frac{4\pi R^3}{3}.$$

Finally, the quenching ratio is given by

$$\frac{I_0}{I} = 1 + \frac{4\pi R_0^6}{3} n_{CuS} \left(n_{PbS} - \frac{4\pi}{3} n_{CuS} \right). \tag{9}$$

By inspection, this shows that a somewhat more realistic treatment of the variance due to FRET leads to a quadratic dependence on quencher concentration and a dependence on the concentration of the donor. However, this treatment does not consider the actual particle distribution, which requires a simulation described below.

c. Random distribution and diffusion. Several factors of quenching by FRET are not included in the FRET radius-only model and crystalline structure model. First, the assumption that CuS NDs are evenly distributed among PbS QDs is invalid in an ideal/hard-sphere solution. Second, the diffusion of species in the solution is not taken into consideration, which could contribute to fluorescence quenching as the FRET rate is nonlinear with the interparticle distance. Since an interparticle distance distribution function is not generally analytic, we carried out a simulation of the quenching behavior using kinetic Monte Carlo (kMC) modeling, considering both the distribution and fluctuation of the interparticle distance and their influence on fluorescence quenching.³⁵ Briefly, PbS QDs and CuS NDs are randomly positioned in the space with a defined number density. Complete matrices composed of FRET rates for every emitter-quencher pair in the ensemble are then calculated and used for the pathway selection process to determine the fate of all emitters. Note that FRET rates between PbS QDs are much smaller than those between PbS QDs and CuS NDs (~104 times slower), and, thus, are excluded from the rate matrices. Finally, the quenching ratio is extracted from the statistics of results (see the supplementary material for details). Diffusion is also implemented in the kMC simulation by a three-dimensional random walk,

$$\mathbf{R}_{N+1} - \mathbf{R}_N = \sqrt{6D\Delta t} \cdot \mathbf{n}_{rand}, \tag{10}$$

where R_i is the position vector of nanocrystals at the *i*th time step, D is the diffusion coefficient, Δt is the time step length limited by the

lifetime of the emitter, and n_{rand} is a random unit vector. It is worth mentioning here that the diffusion coefficients are calculated based on the size parameters obtained from TEM images where surface ligands are invisible, which is a potential source of error in modeling and simulations. This applies to both the Stern–Volmer model and the kinetic Monte Carlo simulations of FRET quenching where diffusion coefficients are used. The introduced deviations, however, are not as significant in the results since the surface ligands oleylamine on both PbS QDs and CuS NDs are inherently angled thus having limited contributions to the hydrodynamic radius. Predictions made based on different models are compared with experimental results (Fig. 3).

B. Simulation results

All models of quenching other than the kMC simulation grossly underestimate the observed quenching behavior at low acceptor densities and do not account for the apparent nonlinear nature of quenching. We can conclude that quenching ratios are underestimated in the Stern–Volmer model, FRET radius, and crystalline structure models, while quenching by FRET with random nanocrystal distribution gives much higher predicted quenching ratios that are comparable to the experimental data. This indicates that randomizing the distribution of nanocrystals in the solution allows part of the PbS QDs to be in the close vicinity of CuS NDs, resulting in very high FRET rates and high probabilities of energy transfer.

The second pattern of quenching observed in experimental data is the non-linear dependence of quenching ratios on quencher concentrations. This is natural when FRET is the mechanism of energy transfer responsible for quenching instead of collision, resulting from the r^{-6} dependence of the FRET rate. It is worth mentioning that the only model that predicts a non-linear dependence is the crystalline defect model. The nonlinearity is not obvious in the range of plotting but is captured at much higher quencher concentrations (see the supplementary material, Fig. S18). Both Stern–Volmer and FRET radius calculations give strictly linear relationships.

Furthermore, distance fluctuations introduced by diffusion contribute to higher quenching ratios and match experimental data more accurately. A brief explanation is as follows: Although the interparticle distance can decrease or increase with diffusion, which will lead to raising or lowering of the FRET rate, respectively, this impact on the FRET rate is clearly different for donor–quencher pairs separated at long distances and those separated at a short distance due to the r^{-6} dependence. This difference in the rate of change is directly reflected in the differential of the r^{-6} function. For donor–quencher pairs that are close in distance, the enhancement in the FRET rate arising from a decreasing distance is more significant than the decay in the FRET rate induced by increasing distance, resulting in an overall higher FRET efficiency; such differences still exist for donor–quencher pairs that are distant away from each other but at a much smaller scale. All taken into consideration,

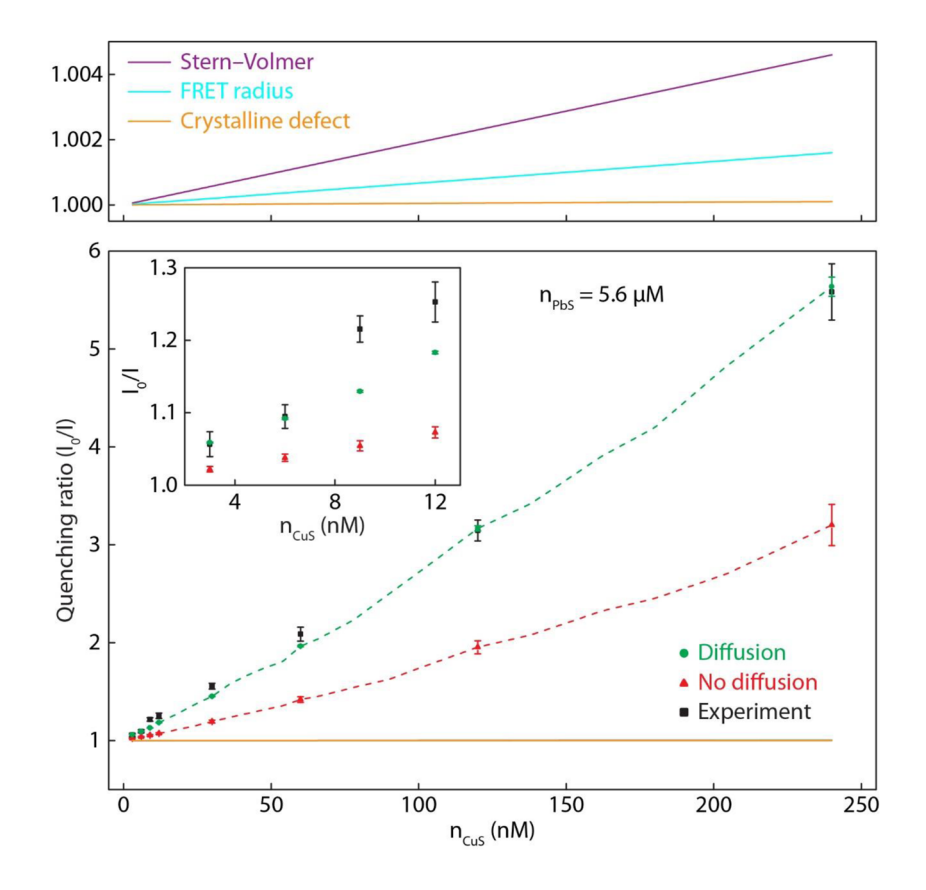
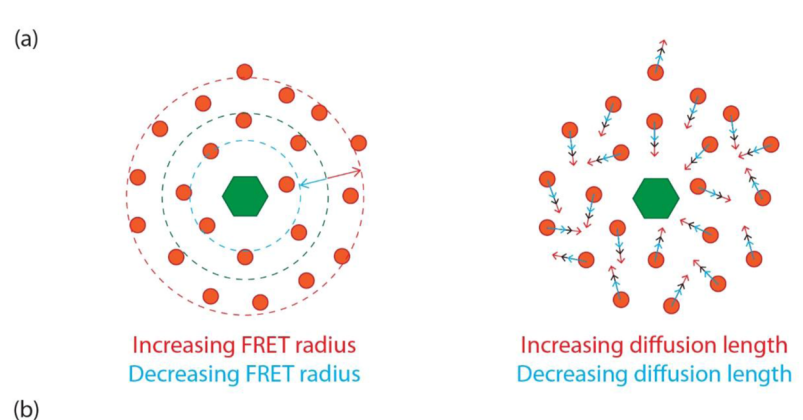


FIG. 3. Comparison of quenching ratio-CuS NDs concentration curves between experiments and models/simulations. Bottom: Full-scale graph. Experimental results squares) and predictions based on random distribution with no diffusion (red triangles) and random distribution with diffusion (green circles) are plotted. The dashed lines are a guide to the eye and show the trend only. Top: Zoomed-in graph at a low quenching ratio. Predictions based on Stern-Volmer (violet), FRET radius (cyan), and crystalline structure (orange) are plotted. Inset: Zoomed-in graph at low guencher concentrations.



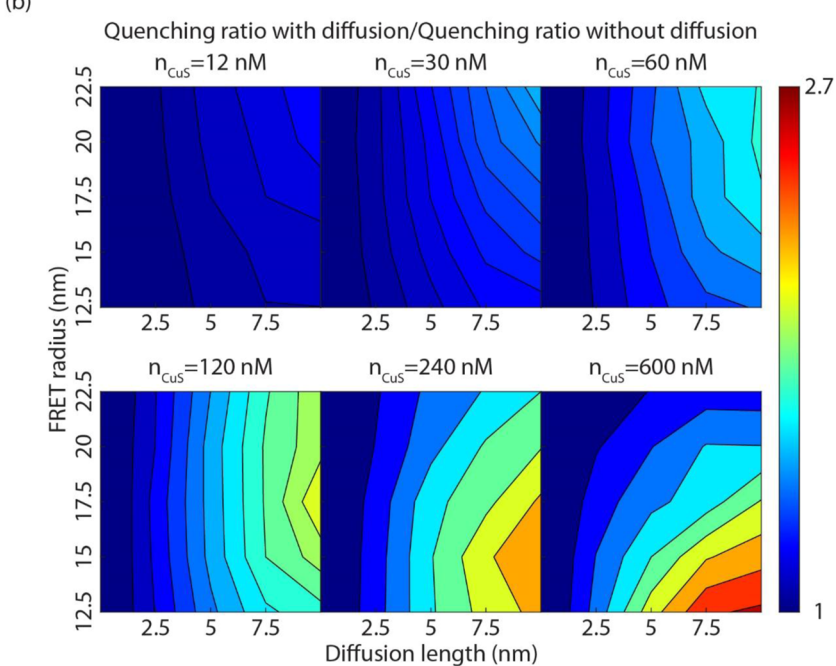


FIG. 4. (a) Schematic demonstration of the changing FRET radius and diffusion length. (b) A color-coded map of the enhancement of the quenching ratio by diffusion with changing diffusion length and FRET radius at different quencher concentrations. The enhancement of the quenching ratio is defined as the ratio between the quenching ratios with diffusion, $(\frac{b_0}{I})_d$, and the quenching ratios without diffusion, $(\frac{b_0}{I})_n$. The diffusion length is defined as $\sqrt{6D\Delta t}$.

in the scheme of quenching by FRET, diffusion has a positive contribution to fluorescence quenching (see the supplementary material for a more detailed discussion).

Besides the clearly observed decrease in the donor lifetime, we also notice a shift in the time-resolved Pl traces from mono-exponential decay to multi-/bi-exponential decay when quenchers are introduced in the titration experiments. Such a transition is not common for canonical quenching pairs but could happen if the quenching rate is non-constant. The non-constant quenching rate is true for our FRET system in the binary solution where the spatial distribution of donors and quenchers makes a significant difference in the FRET rate: donors in the close vicinity of quenchers will rapidly go through the FRET deactivation pathway, while FRET rates for donor-quencher pairs that are more distantly separated will be lower and comparable with other decay rates. This type of quenching behaviors is, indeed, observed in time-resolved PL experiments: at early time, fast decay processes show up in samples with

quenchers added, which are representatives of the rapid FRET rates for donor–quencher pairs at close distances but are not present in pure PbS samples; at a later time, decay processes for quenched samples become slower and more comparable with the decay pattern for pure PbS (see the supplementary material, Fig. S11). Furthermore, our simulations are also capable of capturing this behavior by monitoring the number of quenching events at every time step (see the supplementary material, Fig. S12). Again, a huge number of donors went through the FRET deactivation pathway at a very early time; diffusion then plays a role at later times by increasing the FRET rate for more distantly separated donor–quencher pairs, resulting in more quenching at later times and eventually more quenching in total

We explore how diffusion and the FRET radius interact in Fig. 4. Naturally, the enhancement by diffusion should increase as the diffusion length gets longer, which we observe at all quencher concentrations. However, the impact of FRET radius on

enhancement by diffusion is different and shows a pattern of "saturation of quenching." At low quencher concentrations, diffusion enhances quenching more at elevated FRET radii. At high quencher concentrations and high FRET radii, diffusion does not enhance quenching. We note that the FRET radius is a measurement of the quenching ability for each individual quencher, while quencher concentration reflects the total number of quenchers. When the quencher concentration is low, the number of emitters that all quenchers can access is not saturated; in this case, the higher the FRET radius is, the more emitters reach the interaction region through diffusion, resulting in a higher enhancement. When the quencher concentration is high, most of the emitters are already accessible to quenchers without diffusion especially if the FRET radius is large-hence the "saturation of quenching." For comparison, we carried out similar simulations for a canonical FRET pair (cyanine dyes), and it is clear that the contribution from diffusion is much less significant (see the supplementary material, Fig. S19). In conclusion, the long FRET radius due to large absorption sections of CuS NDs and the random distribution of particles in colloidal solutions gives rise to the high quenching ratio at low quencher concentrations, while also showing that diffusion can play a significant role in the nonlinear enhancement of quenching. Diffusion is not commonly considered in any model of FRET-based quenching, yet should be carefully monitored, especially in systems where the excited state lifetime is long.

III. CONCLUSION

Fluorescence quenching is a canonical method in the study of reacting systems and is used broadly in biological and chemical assays. However, simple applications of Stern-Volmer quenching are not appropriate in FRET pairs, given the nonlinearity of dipole-dipole coupling. Attempts to adapt other FRET models or effective volume approaches also fail to describe quenching. While a more complex behavior can be invoked to explain the quenching behavior, the quantitative agreement between quenching studies and KMC simulations that take into account real interparticle separations and diffusion suggests that a simple general model captures the high magnitude and nonlinearity of quenching in a PbS-CuS system. Therefore, we conclude that non-interacting molecular systems can be effectively quenched with low-concentrations of impurities, provided that energetic conditions are met. Our results suggest that dipolar coupling and diffusion serve to "superpower" quenching, concentrating a diffuse excitation on a few plasmonic defects. These effects will become more important in long-lived excitations in the near and shortwave infrared (where diffusion can play a role) or in materials with high transition dipole moments (where the FRET radius is elevated).

SUPPLEMENTARY MATERIAL

The supplementary material includes the following sections: detailed experimental procedure, TEM analysis, correction for inner filter effect (IFE), lifetime analysis, description of kinetic Monte Carlo (KMC) algorithm, mathematical discussion about the impact of diffusion on quenching, and simulation results for canonical FRET pairs.

ACKNOWLEDGMENTS

This work was supported by the National Science Foundation under Grant No. CHE 1945572. We thank Stephanie Tenney for help with the TEM imaging and Anthony Sica and Ash Hua for help with the lifetime measurements.

AUTHOR DECLARATIONS

Conflict of Interest

The authors have no conflicts to disclose.

Author Contributions

Xuanheng Tan: Conceptualization (equal); Data curation (equal); Formal analysis (equal); Funding acquisition (supporting); Investigation (lead); Methodology (equal); Project administration (equal); Validation (lead); Visualization (lead); Writing – original draft (lead); Writing – review & editing (equal). **Justin R. Caram**: Conceptualization (equal); Formal analysis (equal); Funding acquisition (lead); Methodology (equal); Project administration (lead); Supervision (lead); Writing – original draft (equal); Writing – review & editing (equal).

DATA AVAILABILITY

The data that support the findings of this study are available from the corresponding author upon reasonable request.

REFERENCES

- ¹O. Stern and M. Volmer, "Über die abklingzeit der fluoreszenz," Z. Phys. **20**, 183–188 (1919).
- ²P. K. Behera, T. Mukherjee, and A. K. Mishra, "Simultaneous presence of static and dynamic component in the fluorescence quenching for substituted naphthalene—CCl₄ system," J. Lumin. **65**, 131–136 (1995).
- ³J.-Q. Tong *et al.*, "Probing the adverse temperature dependence in the static fluorescence quenching of BSA induced by a novel anticancer hydrazone," Photochem. Photobiol. Sci. **11**, 1868–1879 (2012).
- ⁴T. Htun, "Excited-state proton transfer in nonaqueous solvent," J. Fluoresc. 13, 323–329 (2003).
- H. S. Geethanjali, D. Nagaraja, R. M. Melavanki, and R. A. Kusanur, "Fluorescence quenching of boronic acid derivatives by aniline in alcohols A negative deviation from Stern–Volmer equation," J. Lumin. 167, 216–221 (2015).
 T. Forster, "Energiewanderung und fluoreszenz," Naturwissenschaften 33, 166–175 (1946).
- ⁷D. N. Ermolenko *et al.*, "Observation of intersubunit movement of the ribosome in solution using FRET," J. Mol. Biol. **370**, 530–540 (2007).
- ⁸J. W. Borst *et al.*, "Structural changes of yellow Cameleon domains observed by quantitative FRET analysis and polarized fluorescence correlation spectroscopy," Biophys. J. **95**, 5399–5411 (2008).
- ⁹J. W. Taraska, M. C. Puljung, N. B. Olivier, G. E. Flynn, and W. N. Zagotta, "Mapping the structure and conformational movements of proteins with transition metal ion FRET," Nat. Methods **6**, 532–537 (2009).
- ¹⁰ X. Dong and D. D. Thomas, "Time-resolved FRET reveals the structural mechanism of SERCA-PLB regulation," Biochem. Biophys. Res. Commun. 449, 196–201 (2014).
- ¹¹ H. Mazal and G. Haran, "Single-molecule FRET methods to study the dynamics of proteins at work," Curr. Opin. Biomed. Eng. **12**, 8–17 (2019).
- ¹²M. Inokuti and F. Hirayama, "Influence of energy transfer by the exchange mechanism on donor luminescence," J. Chem. Phys. 43, 1978–1989 (1965).

- ¹³U. F. Edgal, "Partial nearest neighbor PDF for multi-component material systems," J. Math. Chem. 42, 1101–1134 (2007).
- ¹⁴R. D. Rohrmann and J. Zorec, "Thermostatistical description of gas mixtures from space partitions," Phys. Rev. E 74, 041120 (2006).
- ¹⁵U. F. Edgal, "The exact statistical thermodynamics of classical fluids," J. Chem. Phys. **94**, 8179–8190 (1991).
- ¹⁶P. Sur and B. Bhattacharjee, "nth-Nearest neighbour distribution functions of a binary fluid mixture," J. Chem. Sci. **121**, 929–934 (2009).
- ¹⁷S. Torquato, B. Lu, and J. Rubinstein, "Nearest-neighbor distribution functions in many-body systems," Phys. Rev. A 41, 2059 (1990).
- ¹⁸S. Chan et al., "Monodisperse and size-tunable PbS colloidal quantum dots via heterogeneous precursors," J. Mater. Chem. C 5, 2182–2187 (2017).
- ¹⁹Y. Xie et al., "Metallic-like stoichiometric copper sulfide nanocrystals: Phase-and shape-selective synthesis, near-infrared surface plasmon resonance properties, and their modeling," ACS Nano 7, 7352–7369 (2013).
- ²⁰ P. G. Wu and L. Brand, "Resonance energy transfer: Methods and applications," Anal. Biochem. 218, 1–13 (1994).
- ²¹ A. Einstein, "Über die von der molekularkinetischen Theorie der Wärme geforderte Bewegung von in ruhenden Flüssigkeiten suspendierten Teilchen," Ann. Phys. 322, 549–560 (1905).
- 22 I. Moreels et~al., "Size-dependent optical properties of colloidal PbS quantum dots," ACS Nano 3, 3023–3030 (2009).
- ²³ N. A. Jose, H. C. Zeng, and A. A. Lapkin, "Hydrodynamic assembly of two-dimensional layered double hydroxide nanostructures," Nat. Commun. 9, 4913 (2018).
- ²⁴Y. Liu *et al.*, "Turn-on fluoresence sensor for Hg²⁺ in food based on FRET between aptamers-functionalized upconversion nanoparticles and gold nanoparticles," J. Agric. Food Chem. **66**, 6188–6195 (2018).
- ²⁵ J. Liu and Y. Lu, "FRET study of a trifluorophore-labeled DNAzyme," J. Am. Chem. Soc. 124, 15208–15216 (2002).

- ²⁶L. Albertazzi, D. Arosio, L. Marchetti, F. Ricci, and F. Beltram, "Quantitative FRET analysis with the E⁰GFP-mCherry fluorescent protein pair," Photochem. Photobiol. 85, 287–297 (2009).
- ²⁷ A. M. Dennis and G. Bao, "Quantum dot-fluorescent protein pairs as novel fluorescence resonance energy transfer probes," Nano Lett. 8, 1439–1445 (2008).
- ²⁸I. A. Ahmed, J. M. Rodgers, C. Eng, T. Troxler, and F. Gai, "PET and FRET utility of an amino acid pair: Tryptophan and 4-cyanotryptophan," Phys. Chem. Chem. Phys. **21**, 12843–12849 (2019).
- ²⁹ M. Massey, W. R. Algar, and U. J. Krull, "Fluorescence resonance energy transfer (FRET) for DNA biosensors: FRET pairs and Förster distances for various dye–DNA conjugates," Anal. Chim. Acta 568, 181–189 (2006).
- ³⁰D. C. Torney and H. M. McConnell, "Diffusion-limited reaction rate theory for two-dimensional systems," Proc. R. Soc. London, Ser. A **387**, 147–170 (1983).
- ³¹B. Wallace and P. J. Atzberger, "Förster resonance energy transfer: Role of diffusion of fluorophore orientation and separation in observed shifts of FRET efficiency," PLoS One 12, e0177122 (2017).
- ³²D. Haenni, F. Zosel, L. Reymond, D. Nettels, and B. Schuler, "Intramolecular distances and dynamics from the combined photon statistics of single-molecule FRET and photoinduced electron transfer," J. Phys. Chem. B 117, 13015–13028 (2013).
- ³³S. Chandrasekhar, "Stochastic problems in physics and astronomy," Rev. Mod. Phys. 15, 1–89 (1943).
- ³⁴G. Zou and H.-I. Wu, "Nearest-neighbor distribution of interacting biological entities," J. Theor. Biol. 172, 347–353 (1995).
- $^{\bf 35}$ A. F. Voter, "Introduction to the kinetic Monte Carlo method," in *Radiation Effects in Solids* (Springer, 2007), pp. 1–23.
- ³⁶I. V. Gopich and A. Szabo, "Theory of the energy transfer efficiency and fluorescence lifetime distribution in single-molecule FRET," Proc. Natl. Acad. Sci. U. S. A. **109**, 7747–7752 (2012).
- ³⁷A. Barth *et al.*, "Unraveling multi-state molecular dynamics in single-molecule FRET experiments. I. Theory of FRET-lines," J. Chem. Phys. 156, 141501 (2022).